MOLECULAR INCLUSION REACTIONS BETWEEN METAL COMPLEXES OF AZO COMPLEXONS AND α-CYCLODEXTRIN IN AQUEOUS SOLUTION

Akitoshi SEIYAMA, Noboru YOSHIDA, and Masatoshi FUJIMOTO[*]
Department of Chemistry II
Faculty of Science
Hokkaido University
Sapporo 060
Japan

ABSTRACT.   Kinetics of the molecular inclusion reactions of the azo complexons and their metal complexes with α- and β-cyclodextrins (α- and β-CD$_x$) were studied in aqueous solution by means of a spectrophotometric and a stopped-flow method. The acid dissociation of the azo complexons was regulated by the inclusion with CD$_x$. Two-step process was observed for the interaction of α-cyclodextrin with LH^{*3-} species of the azo complexons and with the metal complexes.

INTRODUCTION

The azo complexons, 3-IDA-5-R-HAB (Fig. 1), which have a coordinating iminodiacetate group, show the conformational change in the acid dissociation[1,2] and the complexation with metal ions.[3] The stability of the inclusion complexes of the azo complexons with α-cyclodextrin (α-CD$_x$) depends on the complementary geometry between the diameter of hydrophobic cavity of α-cyclodextrin and the shape and the size of guest molecule.[4]
In the present paper, we report the stereoselectivity and the regulation of reactivity in molecular inclusion reactions with α-cyclodextrin.
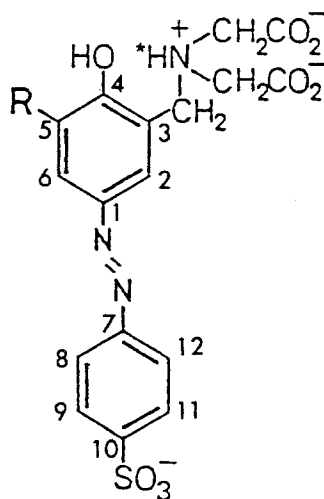

Fig. 1. Structural formula of the azo complexons, p-(3-carboxymethyl-aminomethyl-4-hydroxy-5-alkylphenyl-azo)benzenesulfonic acid (3-IDA-5-Pr-HAB)

EXPERIMENTAL

All chemicals used were of analytical

grade, unless otherwise specified. Water was deionized and distilled.
The azo complexons, 3-IDA-5-R-HAB (R = Me and Pr), were synthesized by
Mannich condensation[5] of p-hydroxyphenylazo derivatives of sulfanilic
acid (HAB) with iminodiacetic acid (IDA) and formaldehyde. The crude
samples of the synthesized 3-IDA-5-R-HAB were purified by cellulose
column chromatography (Avicel Microcrystalline Cellulose, 1-butanol :
2 mol dm^{-3} aqueous NH_3 : ethanol = 60 : 20 : 20, v/v/v). The purities
of the 3-IDA-5-R-HAB were confirmed by elemental analysis, paper
chromatography, absorption spectra, and ^{1}H NMR. Found: C, 49.16; H,
4.16; N, 9.44; S, 7.27% for 3-IDA-5-Me-HAB. Calcd for $C_{18}H_{19}N_3O_8S$: C,
49.54; H, 4.16; N, 9.63; S, 7.35%. Found: C, 46.27; H, 5.84; N, 13.08;
S, 6.40% for 3-IDA-5-Pr-HAB. Calcd for $C_{20}H_{23}N_3O_8S \cdot 3/2NH_3$: C, 48.92;
H, 5.64; N, 12.84; S, 6.50%. Absorption bands for 3-IDA-5-Me-HAB: 354
(ε = 23600) at pH 4.2 and 467.5 nm (ε = 33000 mol^{-1} dm^3 cm^{-1}) at pH 12.7.
Absorption bands for 3-IDA-5-Pr-HAB: 354 (ε = 24000) at pH 4.2 and 477 nm
(ε = 30200 mol^{-1} dm^3 cm^{-1}) at pH 13.3. ^{1}H NMR (TMS/CDCl$_3$) for 3-IDA-5-
Pr-HAB at pD = 9.3: δ 2.51. 1.53, and 0.84 (t, 2H, m, 2H, and t, 3H,
$-CH_2CH_2CH_3$), 4.16 and 3.52 (s, 2H and s, 4H, $-CH_2NH^+(CH_2CO_2^-)_2$), 7.65 and
7.52 (d, 1H and d, 1H, $-C_6H_2R_3R_5O^-$), 7.84 and 7.68 (d, 2H, and d, 2H,
$-C_6H_4SO_3^-$). The purified 3-IDA-5-R-HAB were used as a free acid form.
Cyclodextrins, α- and β-CD$_x$ (Tokyo Kasei), were purified by the method
of Cramer and Henglein using p-cymen, cyclohexane, and fluorobenzene.[6]
A Hitachi-Horiba pH-meter F7-ss was used for the determination of pH
values. Acid dissociation constants were determined spectrophotometri-
cally with a Hitachi 808 spectrophotometer. The absorption spectra were
measured at constant ionic strength, I = 0.1 mol dm^{-3}(NaCl). Kinetic
measurements were carried out with a Union Giken stopped-flow spectro-
photometer RA-401. The 100 MHz ^{1}H NMR spectra were taken on a JEOL JNM-
FX 100 PFT spectrometer.

RESULTS AND DISCUSSION

Equilibria of the Inclusion Reactions and the Acid Dissociation of the
Guest Molecule in the Presence of Cyclodextrin

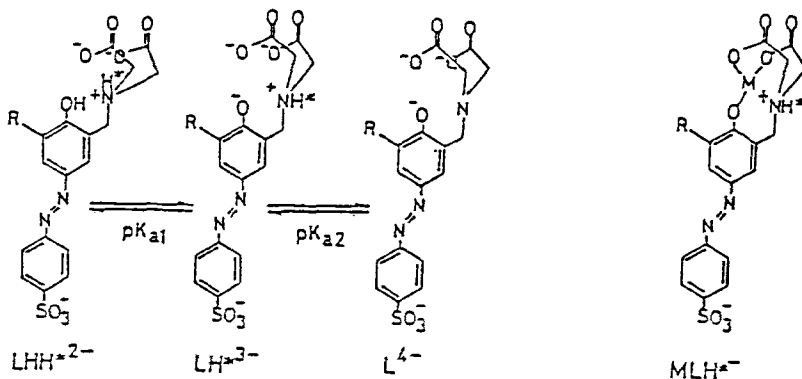Fig. 2. The structure of LHH$*^{2-}$, LH$*^{3-}$, L^{4-}, and MLH$*^{-}$

The absorption spectra of 3-IDA-5-R-HAB at varying CD_x concentrations showed isosbestic points at constant pH and 25 °C. The ligand species, $LHH*^{2-}$, $LH*^{3-}$, L^{4-}, and the metal complexes, $MLH*^-$ (M = Ni and Zn) (Fig. 2), were found to form 1 : 1 inclusion complexes with α- and β-CD_x from the spectrophotometric measurements. Figure 3 shows the spectral change in the formation of the inclusion compound of $NiLH*^-$ (R = Pr) with α-CD_x. Table 1 shows the stability constants of the inclusion complexes of the azo complexons and their metal complexes with α- and β-CD_x.

 The acid dissociation equilibria of the ligand coupled with the inclusion equilibria can be expressed in Schemes 1 and 2, where K_{a1}, K_{a2}, K'_{a1}, and K'_{a2} are the acid dissociation constants of $LHH*^{2-}$, $LH*^{3-}$, $LHH*^{2-}$-CD_x, and $LH*^{3-}$-CD_x, respectively. K, K', and K'' are the stability constants of the inclusion compounds, $LHH*^{2-}$-CD_x, $LH*^{3-}$-CD_x, and L^{4-}-CD_x, respectively. The apparent acid
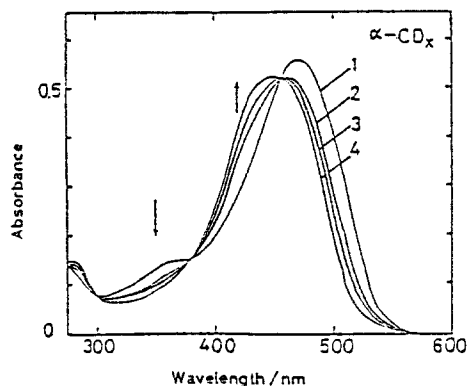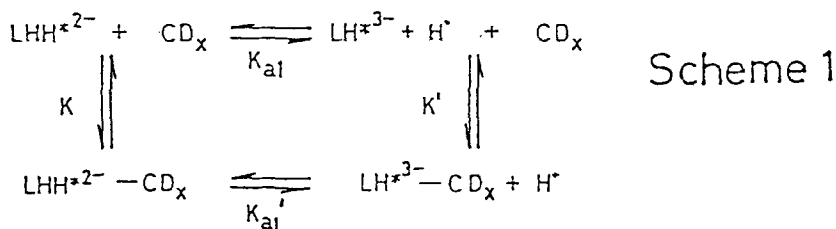

Fig. 3. The spectral change of $NiLH*^-$ (R = Pr) in the presence of α-CD_x: [3-IDA-5-Pr-HAB] = 3.1 x 10^{-5} mol dm^{-3}, [α-CD_x] = 0 (1), 2.0 x 10^{-4} (2), 4.0 x 10^{-4} (3), 8.0 x 10^{-4} mol dm^{-3} (4) at I = 0.1 mol dm^{-3} (NaCl), pH = 4.12, and 25 °C.

Table 1. The Stability Constants of the Inclusion Complexes of the Azo Complexons and their Metal Complexes with α- and β-CD_x

Species	R = Me		R = Pr	
	$K^{\alpha-CD_x}$ mol^{-1} dm^3	$K^{\beta-CD_x}$ mol^{-1} dm^3	$K^{\alpha-CD_x}$ mol^{-1} dm^3	$K^{\beta-CD_x}$ mol^{-1} dm^3
$LHH*^{2-}$	1.6 x 10^3	4.8 x 10^2	2.0 x 10^3	7.7 x 10^2
$LH*^{3-}$	8.3 x 10^3	2.0 x 10^3	8.3 x 10^3	2.6 x 10^3
L^{4-}	1.1 x 10^3	1.3 x 10^2	1.5 x 10^3	2.8 x 10^2
$NiLH*^-$	3.4 x 10^3	1.0 x 10^3	2.0 x 10^3	1.9 x 10^3
$ZnLH*^-$	8.3 x 10^3	2.4 x 10^3	—	—

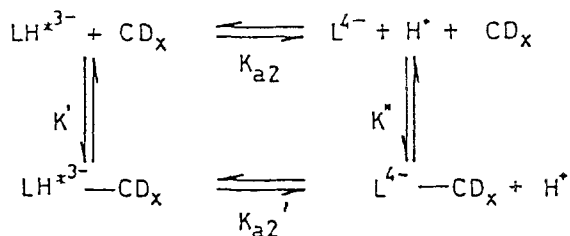At I = 0.1 mol dm^{-3} (NaCl), 25 °C

dissociation constants, $\bar{K}_{a1}$ and $\bar{K}_{a2}$, were determined from the pH-dependence of the absorbance of 3-IDA-5-R-HAB at each CD_x concentration. When the value of $K(K')$ is smaller than that of $K'(K'')$, the value of $p\bar{K}_{a1}$ ($p\bar{K}_{a2}$) decreases as compared with $pK_{a1}(pK_{a2})$. On the contrary when the value of $K(K')$ is larger than that of $K'(K'')$, the value of $p\bar{K}_{a1}$ ($p\bar{K}_{a2}$) increases. As can be seen from Table 1, the inclusion complex, $LH*^{3-}-CD_x$, is considerably stable as compared with $LHH*^{2-}-CD_x$ and $L^{4-}-CD_x$. This indicates that CD_x molecules exert an enhancement effect on the acid dissociation of $LHH*^{2-}$ (Scheme 1). On the contrary, the acid dissociation of $LH*^{3-}$ is retarded in the presence of CD_x (Scheme 2). The values of pK'_{a1} and pK'_{a2} of the guest molecule, 3-IDA-5-Pr-HAB, determined at

$$LHH*^{2-} + CD_x \;\xrightleftharpoons[K_{a1}]{}\; LH*^{3-} + H^{\cdot} + CD_x$$

Scheme 1

$$K \Updownarrow \qquad\qquad K' \Updownarrow$$

$$LHH*^{2-}-CD_x \;\xrightleftharpoons[K'_{a1}]{}\; LH*^{3-}-CD_x + H^{\cdot}$$

$$\bar{K}_{a1} = K_{a1}\,\frac{1 + [CD_x]K'}{1 + [CD_x]K} \qquad (1)$$

$$LH*^{3-} + CD_x \;\xrightleftharpoons[K_{a2}]{}\; L^{4-} + H^{\cdot} + CD_x$$

$$K' \Updownarrow \qquad\qquad K'' \Updownarrow$$

Scheme 2

$$LH*^{3-}-CD_x \;\xrightleftharpoons[K'_{a2}]{}\; L^{4-}-CD_x + H^{\cdot}$$

$$\bar{K}_{a2} = K_{a2}\,\frac{1 + [CD_x]K''}{1 + [CD_x]K'} \qquad (2)$$

Table 2. The Acid Dissociation Constants of 3-IDA-5-Pr-HAB in the Presence of α- and β-CD_x

Host Molecule	pK_{a1}	pK'_{a1}		pK_{a2}	pK'_{a2}	
		obsd	calcd		obsd	calcd
α-CD_x	6.64	6.1 ± 0.05	6.05	11.04	11.7 ± 0.1	11.75
β-CD_x	6.64	6.2 ± 0.05	6.18	11.04	11.7 ± 0.1	11.83

[3-IDA-5-Pr-HAB] = 3.1 x 10^{-5} mol dm^{-3} and [CD_x] = 6.0 x 10^{-3} mol dm^{-3}, are shown in Table 2.

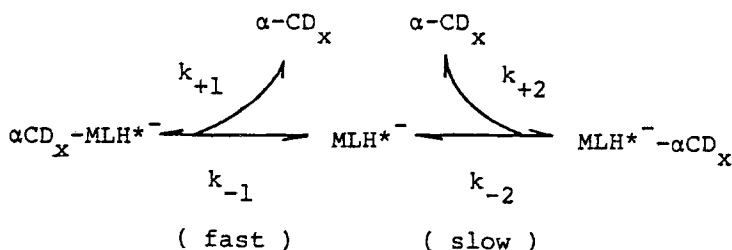## Kinetics of the Inclusion Reactions of the Azo Complexons and their Metal Complexes with α-CD_x

Kinetic data were obtained under pseudo-first-order conditions in the presence of a large excess of α-CD_x. The inclusion reactions with β-CD_x were too fast to measure by the stopped-flow method. The values of the rate constants are summarized in Table 3. The two-step process was observed in the formation of $LH*^{3-}$-αCD_x and $MLH*^-$-αCD_x. Figure 4 shows the plots of the observed rate constants, k_a and k_b, for the fast and the slow processes respectively against the total α-CD_x concentration, [α-CD_x]. From the dependence of k_a and k_b on [α-CD_x], two types of reaction Schemes, 3 and 4, can be considered.

The relationships between $k_a(k_b)$, $k_{+1}(k_{+2})$ and $k_{-1}(k_{-2})$ are then given by Eqs. 3 and 4 for the reaction Schemes 3 and 4, respectively.

Table 3. The Rate Constants for the Inclusion Reactions
of the Azo Complexons and their Metal Complexes
with α-CD_x

Guest Molecule		k_+ $mol^{-1}dm^3s^{-1}$	k_- s^{-1}
$LHH*^{2-}$	slow	4.6 x 10^2	0.64
$LH*^{3-}$	fast	8.5 x 10^3	16
	slow	1.1 x 10^3	0.56
L^{4-}	slow	1.5 x 10^2	0.26
$NiLH*^-$	fast	9.6 x 10^3	14
	slow	6.4 x 10^2	0.23
$ZnLH*^-$	fast	1.1 x 10^4	12.4
	slow	8.5 x 10^2	0.23

At 25° C, I = 0.1 mol dm^{-3} (NaCl)

$$\alpha\text{-CD}_x \qquad \alpha\text{-CD}_x$$

$$k_{+1} \qquad\qquad k_{+2}$$

$$\alpha CD_x\text{-MLH*}^- \xrightleftharpoons{} MLH*^- \xrightleftharpoons{} MLH*^-\text{-}\alpha CD_x$$

$$k_{-1} \qquad\qquad k_{-2}$$

(fast)   (slow)

Scheme 3

$$\alpha\text{-CD}_x \qquad\qquad \alpha\text{-CD}_x$$

$$k_{+1} \qquad\qquad k_{+2}$$

$$MLH*^- \xrightarrow{} \alpha CD_x\text{-MLH*}^- \xrightarrow{} MLH*^-\text{-}\alpha CD_x$$

$$k_{-1} \qquad\qquad k_{-2}$$

$$\alpha\text{-CD}_x$$

(fast)   (slow)
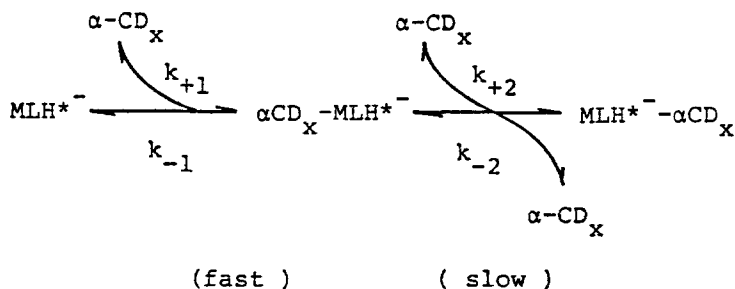
Scheme 4

$$k_a = k_{+1}[\alpha\text{-CD}_x] + k_{-1}$$

$$k_b = k_{-2} + k_{+2}K_{-1}[\alpha\text{-CD}_x]/([\alpha\text{-CD}_x] + K_{-1}) \tag{3}$$

$$k_a = k_{+1}[\alpha\text{-CD}_x] + k_{-1}$$

$$k_b = k_{-2}[\alpha\text{-CD}_x] + k_{+2}[\alpha\text{-CD}_x]^2/([\alpha\text{-CD}_x] + K_{-1}) \tag{4}$$

The dependence of k_a and k_b on $[\alpha\text{-CD}_x]$ under the experimental conditions can be explained only by Eq. 3. The plot of $1/(k_b - k_{-2})$ vs. $1/[\alpha\text{-CD}_x]$ of Eq. 3 gave a straight line with a slope $1/k_{+2}$ and an intercept $1/(k_{+2}K_{-1})$. The value of K_{-1} obtained from the intercept was fairly in good agreement with the value of K_{-1} determined as the ratio of k_{-1}/k_{+1}.

The fast step would be attributed to the inclusion at A-site (see Fig. 5) and the slow step at B-site (see Fig. 6) as judged by the magnitude of the rate constants (Table 3) and ^{1}H NMR spectral criteria.[7] On the other hand the inclusions of LHH*[2-] and L[4-] with $\alpha\text{-CD}_x$ takes place only at B-site.[8]

From the temperature-dependency of the rate constants for the inclusion reactions of the ligand, LH*[3-], and the Ni(II) complex, NiLH*[-], thermodynamic parameters and activation parameters were determined. The
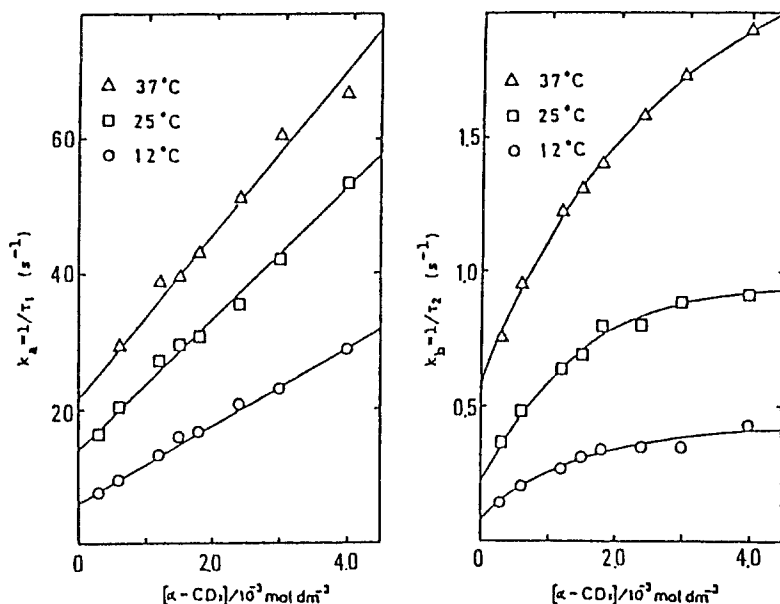
Fig. 4. Dependence of k_a and k_b on $[\alpha\text{-CD}_x]$
$[\text{3-IDA-5-R-HAB}] = 3.0 \times 10^{-5}$ mol dm^{-3}
$[\text{NiCl}_2] = 1.8 \times 10^{-4}$ mol dm^{-3}
at $I = 0.1$ mol dm^{-3}, pH=4.12 and 25 °C. $\lambda_{obs} = 500$ nm

inclusion equilibria are almost enthalpy-controlled; the entropy change ($\Delta S° < 0$) of slow step contributes unfavorably to the formation of the $\alpha\text{-CD}_x$ inclusion complxes. The contribution of the entropy of activation, $\Delta S_+^{\ddagger}$, to the Gibbs energy of activation, $\Delta G_+^{\ddagger}$, in the forward reaction is much larger than that of $\Delta S_-^{\ddagger}$ to $\Delta G_-^{\ddagger}$ in the backward reaction. The entropy term, $\Delta S_+^{\ddagger}$, contributes unfavorably to the Gibbs energy term, $\Delta G_+^{\ddagger}$. This suggests that the hydrophobic interaction does not play an important role in the transition state of the inclusion reactions.
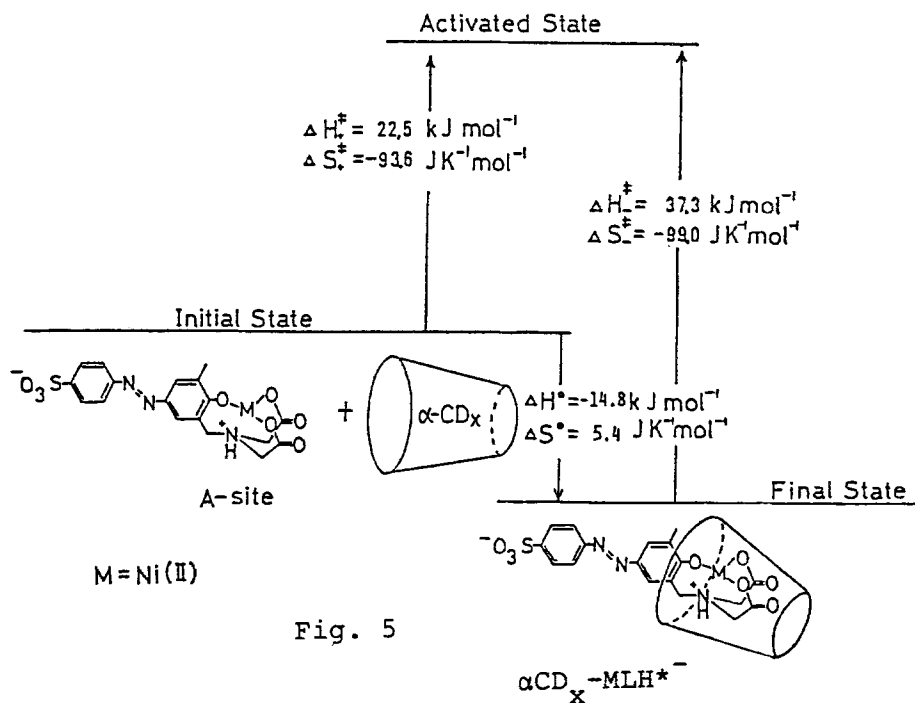
Activated State

$\Delta H_+^{\ddagger} = 22.5 \ kJ \ mol^{-1}$
$\Delta S_+^{\ddagger} = -93.6 \ JK^{-1}mol^{-1}$

$\Delta H_-^{\ddagger} = 37.3 \ kJ \ mol^{-1}$
$\Delta S_-^{\ddagger} = -99.0 \ JK^{-1}mol^{-1}$

Initial State

$\Delta H^{\circ} = -14.8 \ kJ \ mol^{-1}$
$\Delta S^{\circ} = 5.4 \ JK^{-1}mol^{-1}$

A-site

Final State

M = Ni(II)

Fig. 5

$\alpha CD_x - MLH^{*-}$

Activated State

$\Delta H_+^{\ddagger} = 26.7 \ kJ \ mol^{-1}$
$\Delta S_+^{\ddagger} = -102.0 \ JK^{-1}mol^{-1}$

$\Delta H_-^{\ddagger} = 59.8 \ kJ \ mol^{-1}$
$\Delta S_-^{\ddagger} = -56.6 \ JK^{-1}mol^{-1}$

Initial State

$\Delta H^{\circ} = -33.1 \ kJ \ mol^{-1}$
$\Delta S^{\circ} = -45.4 \ JK^{-1}mol^{-1}$

B-site
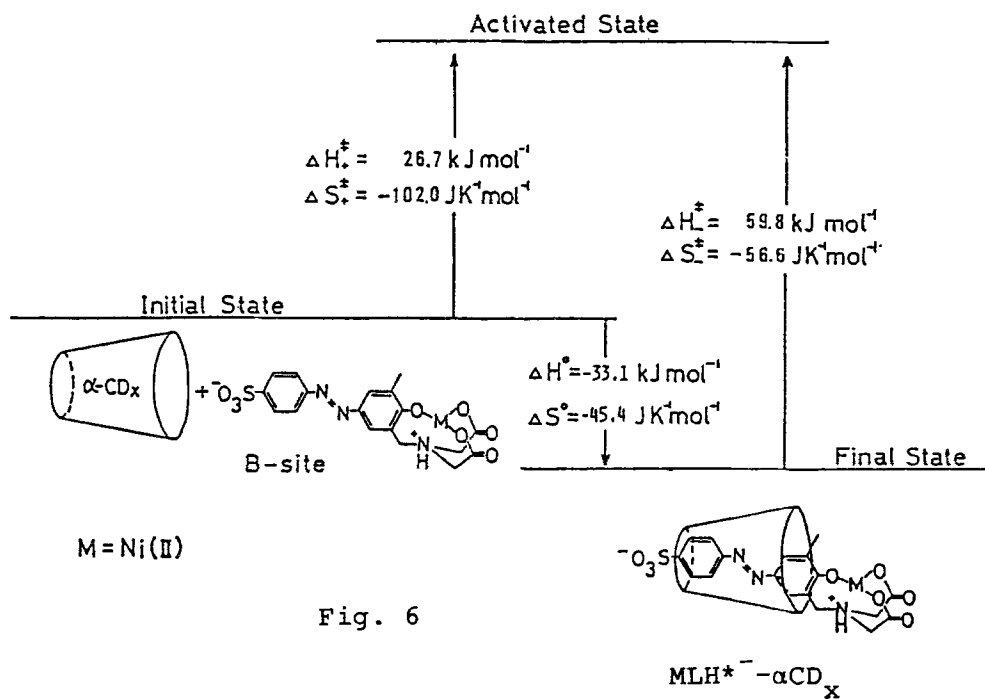
Final State

M = Ni(II)

Fig. 6

$MLH^{*-} - \alpha CD_x$

References

1) For 3,3'-[bis(carboxymethyl)aminoethyl]-o-cresol-sulfonphthalein (Xylenol Orange). S. Nakada, T. Ito, M. Yamada, and M. Fujimoto, Bull. Chem. Soc. Jpn., 54, 2913 (1981).

2) For ethylenediaminetetraacetic acid and related substances. D. Chapman, D. R. Lloyd, and R. H. Prince, J. Chem. Soc., 1963, 3645.

3) Unpublished data; the azo complexons form stable and colored 1 : 1 protonated complexes with bivalent metal ions, Ni(II), Zn(II), and Cu(II), in a weakly acidic solution.

4) M. L. Bender and M. Komiyama, 'Cyclodextrin Chemistry,' Springer-Verlag, 1978; N. Yoshida and M. Fujimoto, Chem. Lett., 1980, 231; N. Yoshida and M. Fujimoto, Chem. Lett., 1980, 1377; N. Yoshida and M. Fujimoto, Bull. Chem. Soc. Jpn., 55, 1039 (1982), and N. Yoshida, A. Seiyama, and M. Fujimoto, Chem. Lett., 1984, 703.

5) J.Körbl and R. Přibil, Chem. Ind. (London), 1957, 233.

6) F. Cramer and F. M. Henglein, Chem. Ber., 91, 308 (1958).

7) The ^{1}H NMR study showed that α-CD_x interacts with the azo-sulfanilate moiety. The downfield shifts of the signals of H_8, H_9, H_{11}, and H_{12} protons by the inclusion into α-CD_x cavity were very large as compared with those of H_2, H_{3a-3b}(methylene groups), H_{5a-5c}(R:propyl group), and H_6.

8) The inclusion at A-site takes place only when the motional freedom of the iminodiacetate group in LH^{*3-} is frozen owing to the formation of the intramolecular hydrogen bond between the amino proton(NH^+), the phenolate($-O^-$), and two carboxylate($-COO^-$) groups of the ligand. This freezing of the motional freedom of the iminodiacetate group in MLH^{*-} is observed in the complexation of metal ions with these donor groups of the ligand.